

Networks of High Performance Trieboelectric Nanogenerators Based on Liquid–Solid Interface Contact Electrification for Harvesting Low-Frequency Blue Energy

Xiaoyi Li, Juan Tao, Xiandi Wang, Jing Zhu, Caofeng Pan,* and Zhong Lin Wang

Blue energy harvested from the ocean is an important and promising renewable energy for the sustainable development of society. Trieboelectric nanogenerators (TENGs) are considered one of the most promising approaches for harvesting blue energy. In this work, a liquid–solid-contact trieboelectric nanogenerator (LS TENG) is fabricated to enhance the friction and magnify energy output by 48.7 times, when compared with the solid–solid-contact TENG with the same area. The buoy-like LS TENG can harvest energy from different types of low-frequency vibration (including up–down, shaking, and rotation movements). Moreover, the outputs of the LS TENGs network can reach 290 μA , 16 725 nC, and 300 V, and the LS TENGs network can directly power hundreds of LEDs and drive a radio frequency emitter to form a self-powered wireless save our souls (SOS) system for ocean emergencies. This work renders an innovative and effective approach toward large-scale blue energy harvesting and applications.

1. Introduction

Energy crisis has become one of world's most serious challenges, as the rapid growth of the total energy consumption. The renewable energies, containing solar,^[1] wind,^[2] geothermal energy,^[3] bio-fuel and so on,^[4] have been intensively explored and converted into electricity to ensure the sustainable development.^[5,6] Especially, the energy harvested from ocean, which is also called blue energy, is inexhaustible and convenient,^[7,8] as water covers more than 70% of the surface of the earth.^[9] Meanwhile, the immense blue energy is independent of season, circadian rhythm, and weather.^[10] However, it is a huge challenge to widely harvest the blue energy based on the heavy, expensive, and

inefficient electromagnetic generators.^[9,11] Fortunately, trieboelectric nanogenerators (TENGs), which are lightweight, cheap, and high efficiency, have achieved tremendous progress in harvesting the ocean blue energy for the past few years.^[12–16]

Nevertheless, most of the blue-energy-harvesting TENGs are based on the friction between solids.^[13,14,17–19] Because of the roughness of the surface and the inefficient contact condition,^[20] the contact/friction area is only a tiny portion of the total surface. Therefore, we design a liquid–solid-contact (LS) buoy trieboelectric nanogenerator, with four key merits, to meet the requirements and harvest the blue energy from ocean. First of all, the sufficient liquid–solid contact will largely increase the friction area and therefore enhance the LS TENG's energy outputs compared with the solid–solid-contact (SS) TENG with the same area. Second, the buoy LS TENG can generate several sequential damping signals just by one pulse of triggering, demonstrating the maximum utilization of the vibration energy. This characteristic merit renders it available for the buoy LS TENG to collect the low-frequency energy sufficiently. Additionally, the buoy LS TENG can acquire energy from different types of movements, including the up–down, shaking, and rotation movements. The last but not the least, the network of buoy LS TENGs could harvest large quantities of energy, including surface wave energy and submarine current energy, to power portable electric devices or navigation systems. In this work, the electricity energy generated from the LS TENGs is stored in the capacitor to drive a wireless save our souls (SOS) radio frequency (RF) transmitter for ocean emergencies. This


Dr. X. Li, J. Tao, Dr. X. Wang, Prof. C. F. Pan, Prof. Z. L. Wang
CAS Center for Excellence in Nanoscience
Beijing Key Laboratory of Micro-Nano Energy and Sensor
Beijing Institute of Nanoenergy and Nanosystems
Chinese Academy of Sciences
Beijing 100083, P. R. China
E-mail: cfpan@binn.cas.cn

Dr. X. Li, J. Tao, Dr. X. Wang, Prof. C. F. Pan, Prof. Z. L. Wang
School of Nanoscience and Technology
University of Chinese Academy of Sciences
Beijing 100049, P. R. China

Dr. X. Li, Prof. J. Zhu
National Center for Electron Microscopy in Beijing
School of Materials Science and Engineering
The State Key Laboratory of New Ceramics and Fine Processing
Key Laboratory of Advanced Materials (MOE) and Center for
Nano and Micro Mechanics
Tsinghua University
Beijing 100084, China

Prof. C. F. Pan, Prof. Z. L. Wang
Center on Nanoenergy Research
School of Physical Science and Technology
Guangxi University
Nanning, Guangxi 530004, P. R. China

Prof. Z. L. Wang
School of Materials Science and Engineering
Georgia Institute of Technology
Atlanta, GA 30332-0245, USA

 The ORCID identification number(s) for the author(s) of this article can be found under <https://doi.org/10.1002/aenm.201800705>.

DOI: 10.1002/aenm.201800705

work provides a more efficient method of capturing the blue energy and expands its applications.

2. Results and Discussion

A buoy-like liquid–solid-contact TENG (in **Figure 1** and **Figure S1**, Supporting Information) is fabricated to capture the low-frequency water wave energy. It could be made of conventional materials, such as polytetrafluoroethylene (PTFE), fluorinated ethylene propylene (FEP), nylon, polyethylene terephthalate (PET), polydimethylsiloxane (PDMS), and electrodes (copper, silver, or aluminum). Such materials are not only low-cost and lightweight but also enduring for ten or more years in a sealed unit in the ocean. The buoy-like LS TENG in **Figure 1c** contains the outer TENG O1 (with the bottom electrode outside) and the inner TENGs (I1 to I5 with the bottom electrode inside

of the buoy). Under up–down movement, the LS TENG can harvest ambient wave energy into electricity,^[21] with the finite element method simulation illustrated in **Figure S1c** in the Supporting Information. While under shaking or rotation movement, the inner TENGs from I1 to I5 are connected in parallel to collect the mechanical energy of the inner liquid (e.g., water).

The network of triboelectric nanogenerators could convert large quantities of mechanical energy into electricity to supply portable electric devices, navigation systems, or even a town.^[22] Theoretically, a square kilometer with a 3D network of devices spaced at 10 cm intervals could easily generate enough electricity for a town.^[9] Furthermore, the energy harvested from the ocean could be applied in breaking down water for hydrogen fuel, powering the LEDs or sensors, purifying dirty or saline water, and even preventing the metal corrosion. Meanwhile, the network of the buoy TENGs could also be integrated with the wind turbines or solar panels, yielding a multitype power plant.

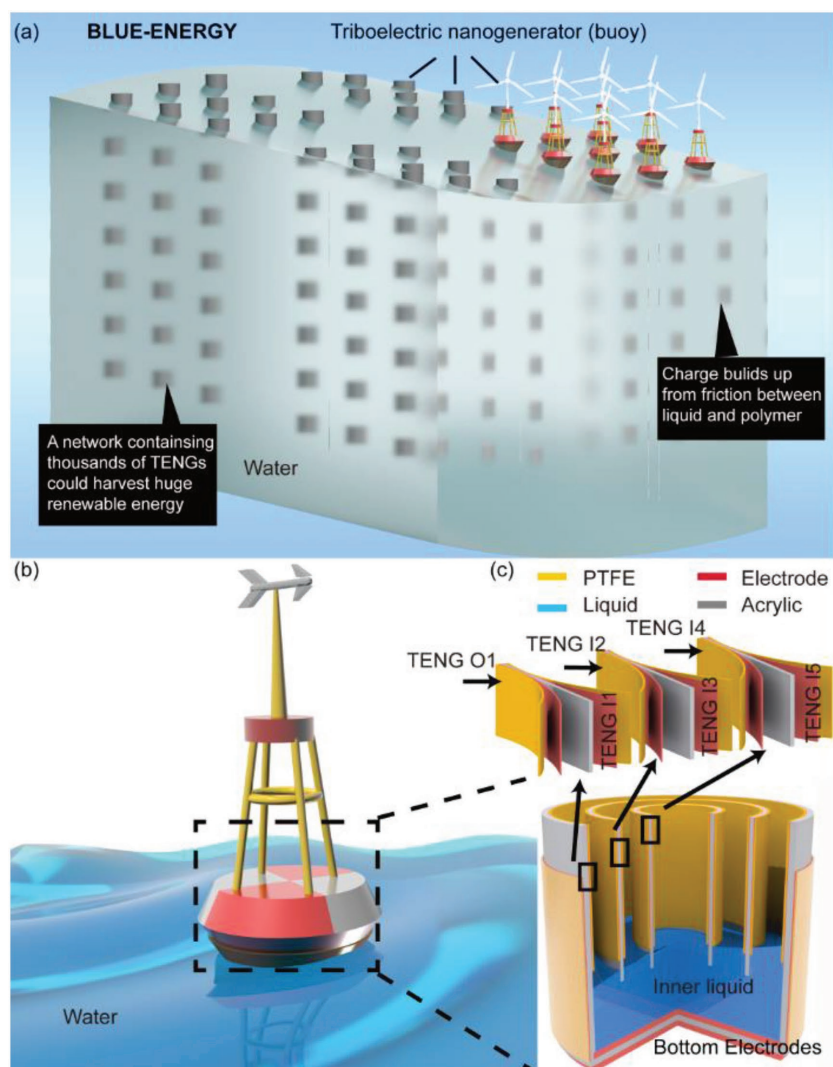


Figure 1. The blue energy harvested by the network of the liquid–solid-contact buoy triboelectric nanogenerators. a) The schematic illustration of the TENG network which contains thousands of single units. b) The structure of a buoy. c) The buoy contains an inner liquid and several polymer films, which function as several TENGs.

2.1. Acquiring Energy from Different Types of Movement

When the LS TENG moves up and down as shown in **Figure 2a**, the PTFE film rubs with the water, generating induced charges on polymer's surface. And the induced potential difference between the two electrodes (bottom electrode and the electrode backside of the PTFE) will drive the electrons to run from the back electrode to the bottom electrode via the external circuit. The schematic working principle is shown in **Figure S2a** in the Supporting Information. A single LS TENG with one PTFE film (8 cm × 10 cm) can produce a considerable output, and its short-circuit current I_{sc} , transferred charge Q_{sc} , and the open-circuit voltage V_{oc} are 40 μ A (**Figure 2b**), 1000 nC (**Figure 2c**), and 400 V (**Figure 2d**) respectively! A single LS TENG can light up nearly 100 LEDs, seen in **Movies S1** and **S2** in the Supporting Information.

Under the shaking or rotation movement (**Figure 2e**), the inner liquid shakes inside the buoy and contacts with the polymer film, resulting the friction charges on the contact surface and the induced potential difference between the two electrodes (the inside bottom electrode and the PTFE film's backside electrode). The schematic working principle is shown in **Figure S2b,c** in the Supporting Information. The short-circuit current, transferred charges, and the open-circuit voltage are 3 μ A, 400 nC, and 120 V, respectively, as shown in **Figure 2f–h**.

The output energy per cycle could not be described simply as the product of I_{sc} and V_{oc} because the pulsed short-circuit current relies on the transferred charge and the contact-separation velocity, as illustrated in **Equation (1)**.

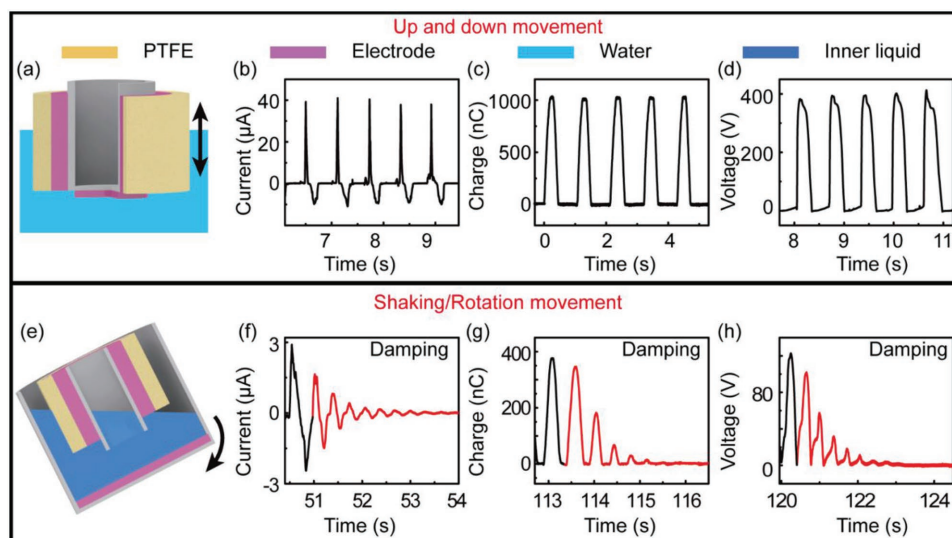


Figure 2. The output signals of the solid–liquid-contact buoy TENG of different movements. a) A schematic diagram of the liquid–solid TENG when moving up and down. b) Short-circuit current, c) transferred charges and d) open-circuit voltage signals of the liquid–solid TENG. e) A schematic diagram of the liquid–solid TENG when shaking or rotating. f) Short-circuit current, g) transferred charges, and h) open-circuit voltage signals of the inner liquid–solid TENG.

$$I_{sc} = \frac{dQ_{sc}}{dt} = \frac{dQ_{sc} \times v}{dx} \quad (1)$$

The generated output energy per cycle could be computed by Equation (2).

$$E_{out} = \int I^2 R dt = \oint V dQ \quad (2)$$

Therefore, the integral of current square, transferred charges, and the voltage are extremely vital and momentous to describe the TENG's output properties. Meanwhile, the velocity/frequency of water waves in the marine environment is uncontrollable, tremendous transferred charges of the friction, instead of big currents, can present appreciable energy outputs.

2.2. Liquid–Solid Interface Contact Electrification to Harvest Low-Frequency Vibration Energy

It should be emphasized that the buoy TENG is especially suitable for efficiently harvesting low-frequency vibration energy. It can be observed that the device has the ability to generate several damping output signals by one pulse of triggering. The figures (Figure 2f–h) all demonstrate that the output signals will last for about eight cycles and gradually damp to zero even after the outer triggering ceases. It implies that the buoy LS TENG has the capability of storing the unabsorbed mechanical energy and gradually converting it into electricity afterward.^[23] In addition, a comparison of LS TENG and SS TENG under different ambient vibration of 0.5, 1, and 2 Hz are carried, demonstrated in Figure S3a,b in the Supporting Information.

The results provide a clear conclusion that the LS TENG generates more distinguishable current peaks than the SS TENG when under the same ambient triggering frequency. Under the frequency of 2 Hz over a short time domain of 10 s, the number of peaks from LS TENG in Figure S3a in the Supporting Information is 36, which is nearly two times as the 20 of SS TENG in Figure S3b in the Supporting Information. This unique characteristic of LS TENG can make the most use of the vibration energy and greatly enlarge the outputs in real circumstance, considering the randomness and low-frequency motion of water waves.

The most significant merit of the LS TENG is that the liquid–solid contact makes the friction more effective and greatly increases the outputs. In the microscale, the contact between solid and solid is insufficient as a consequence of the rugged solid surface. Compared with the liquid–solid contact,^[24] the contact area of solid–solid occupies only a tiny portion of the total surface area (Figure 3). Therefore a contrast experiment has been made, as an LS TENG and sealed SS TENGs are putted in water to collect the wave energy. The output energy in one cycle can be figured out by Equation (2) as $E_{LS} = 2.95 \text{ e}^{-4} \text{ J}$

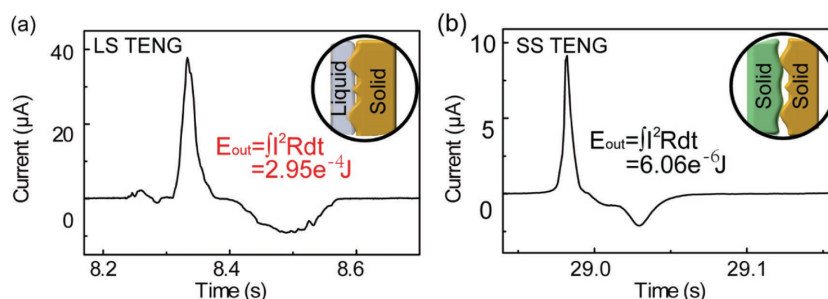


Figure 3. The comparison between liquid–solid TENG and solid–solid TENG. a) The short-circuit current of LS TENG. The inset is the schematic of liquid–solid interface. b) The short-circuit current of SS TENG. The inset is the schematic of solid–solid interface.

Table 1. The properties of the TENGs based on different materials and the merit of the liquid–solid TENGs.

Materials	T	Size [cm ²]	Q _{sc} [nC]	I _{sc} [μA]	V _{oc} [V]	E _{out} = ∫I ² Rdt [μJ per cycle]	E _{out} = ∫VdQ [μJ per cycle]	E _{ave} [μJ cm ⁻² per cycle]
PTFE and Water	L/S	80.0	1000	40	400	295	–	3.68
FEP and Water ^[16]	L/S	30.0	200	10	200	107	–	3.57
Kapton and Hg ^[25]	L/S	15.0	645	9.0	600	≤149	–	≤9.93
FEP and Cu ^[18]	S/S	≈31.8	275	≤21	490	–	≤34.8	≤1.09
FEP and Al ^[35]	S/S	35.0	390	–	19.2	–	≤8.75	≤0.25
FEP and Al ^[36]	S/S	67.2	34.5	–	120	–	1.99	0.03
FEP and Cu ^[37]	S/S	16.0	161	–	470	–	≤20.1	≤1.25
PTFE and Al ^[13]	S/S	≈128	–	50	180	82.8	–	≈0.65
PTFE and Cu ^[17]	S/S	≈5.10	7.20	5.8	17.0	–	≤0.05	≈0.01
PTFE and Cu ^[14]	S/S	98.0	162	46	458	≤70.0	–	0.71

and $E_{SS} = 6.06 \text{ e}^{-6} \text{ J}$, as exhibited in Figure 3a,b. The output energy per cycle of LS TENG is 48.7 times larger than that of SS TENG, which means the LS TENG will generate more electricity energy than SS TENG in same condition. Corresponding to other related works, similar experimental consequence can be acquired to support this phenomenon, as shown in Table 1. Figure S3c–e in the Supporting Information demonstrates the currents, voltages, and charges of PTFE/Water, PTFE/Al, PTFE/Cu, PTFE/PDMS, and PTFE/Kapton with the same size of 80 cm². And the schematic diagram of the comparison

LS and SS TENGs are shown in Figure S4 in the Supporting Information.

2.3. LS TENG with Different Materials

Different types of polymers and different inner liquids are utilized to further demonstrate the performance of LS TENG in Figure 4. We measure the LS TENG output performance based on pure water and various polymers (Figure 4a–c), including

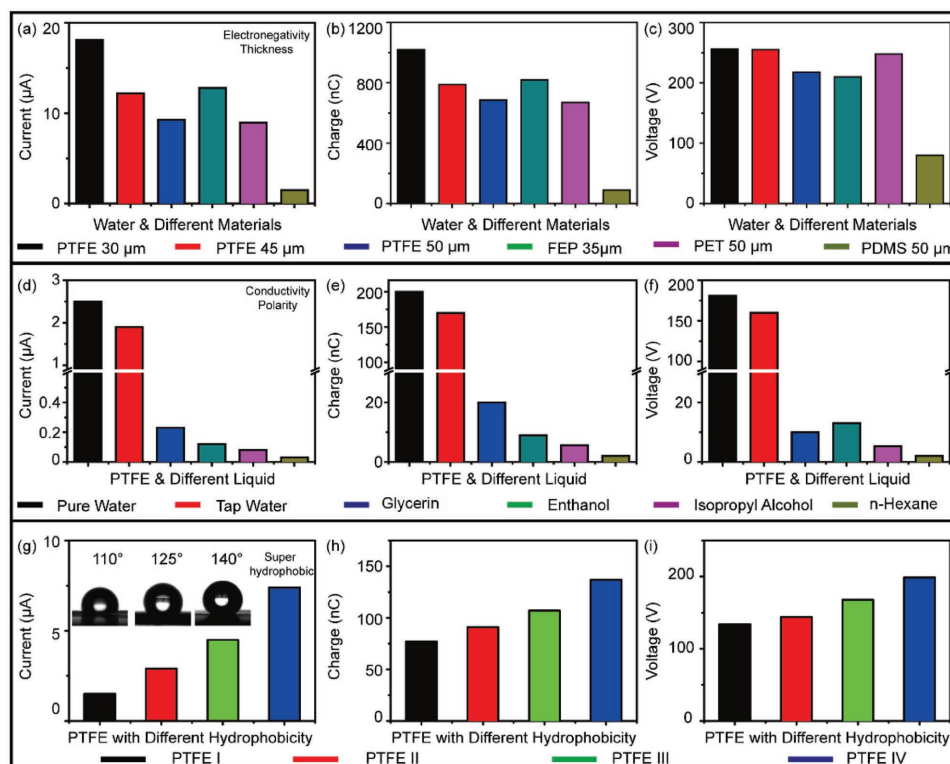


Figure 4. Output performances of the LS TENG with different friction materials. a) The short-circuit current, b) the transferred charges, and c) the open-circuit voltage performances of LS TENGs based on different polymer materials. d) The short-circuit current, e) the transferred charges, and f) the open-circuit voltage performances of LS TENGs based on different liquids. g) The short-circuit current, h) the transferred charges, and i) the open-circuit voltage performances of the LS TENG with different surface hydrophobicity.

PTFE, FEP, PET, and PDMS, and also test the output performance based on PTFE and different liquids (Figure 4d–f), including pure water, tap water, glycerin, ethanol, isopropyl alcohol, and *n*-hexane. According to the signals of PTFE films with 30, 40, and 50 μm thickness, it can be concluded that the outputs, especially the current and the charge, rely on the film thickness.^[25] As the PTFE thickness increases, the output current descends from 18 to 9.3 μA and the charge reduces from 1000 to 700 nC. This phenomenon is due to the increase of induction distance, which is corresponding to some related works.^[15] PTFE's outputs are slightly higher than those of FEP or PET, but obviously higher than the outputs of PDMS. Different polymers with different capable of attracting the electrons (electronegativity) will induce different charges and outputs. Meanwhile, some water still remains on the sticky PDMS's surface when separating, which reduces the practical friction area and causes the low output of PDMS.

The LS TENG based on PTFE (30 μm thickness) with different liquids is also tested. According to the outputs of pure water and tap water, pure water has the higher outputs because of its lower conductivity.^[15] When the conductivity of the water increases, the potential between the two electrodes will enlarge the leak current through the water and thus decrease the output current through extern circuit. It is worth noting that high polarity of the liquid will generate more friction charges and thus cause big output signals (comparing with water, glycerin, ethanol, isopropyl alcohol, and *n*-hexane).^[16,25,26] Meanwhile, the surface hydrophobicity also affects the LS TENG's output signals, as shown in Figure 4g–i. PTFE I and II are bought with different hydrophobicity, and PTFE II is etched by inductively coupled plasma (ICP) to create nanowires on the surface to become PTFE III and IV. After etched for 45 s, PTFE III with many pits on the surface (Figure S5d, Supporting Information) becomes more hydrophobic (140° contact angle) and then generates bigger signals than PTFE II. There are so many nanowires on the surface of PTFE IV (etching time 7 min) that the water drop cannot be adhered to the film, as shown in Movie S3 in the Supporting Information. It can be concluded that the more hydrophobic the PTFE is the bigger output signals it will generate. More details can be seen in Figure S5 in the Supporting Information.

2.4. LS TENG Network for Blue Energy

The network of LS TENG can not only harvest the water wave energy on ocean surface but also the subsurface current, depicted in Figure S6 in the Supporting Information. As the LS TENG can make the most use of the vibration energy and greatly enlarge the outputs, the network of LS TENG could harvest large quantities of energy and have

wide applications, e.g., powering the LEDs,^[27–29] preventing the metal corrosion,^[10] sensing, and purifying sea water.^[30,31] As shown in Figure S6c in the Supporting Information, there are more rusts on the metal's surface (Q235 carbon steel) without LS TENG's protection than that with protection after immersed in sea water for 4 h.^[32]

To exhibit the law of the LS TENG network for harvesting blue energy from ocean, a further experiment is conducted to measure the relationship between the outputs and the unit numbers. Therefore, a small network with 18 PTFE films is fabricated (corresponding to 18 LS TENGs). The output currents and charges of the LS TENG are respectively demonstrated in Figure 5a–d when the unit number *n* is 2, 6, 10, 14, and 18. The current output when *n* = 2 is about 40 μA , which is substantially enhanced to about 290 μA when *n* = 18, as presented in Figure 5a. Figure 5b shows that the current output has an exact linear relation with the unit number. The transferred charges and voltage (Figure S6d, Supporting Information) of the LS TENG network could be as high as 16 725 nC and 300 V, respectively. Also a linear relationship is discovered between the charge and the unit number, as shown in Figure 5d. The charge density and the current density based on the number of units are shown in Figure S6e,f in the Supporting Information. Because

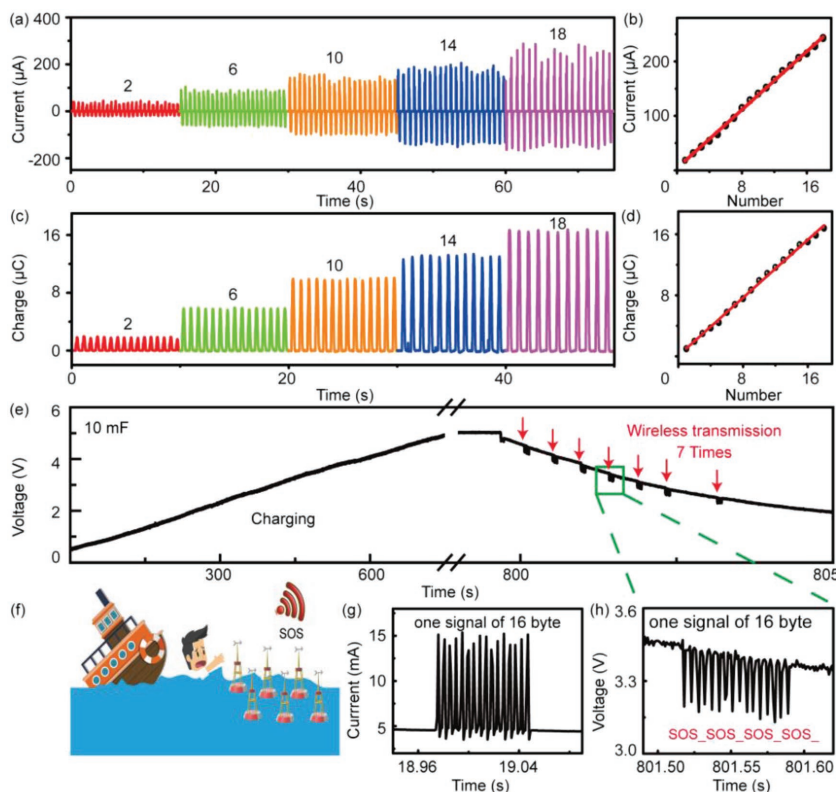


Figure 5. Demonstration of the LS TENG network as a self-powered wireless SOS system. a) The short circuit current of the LS TENG network with the unit number *n* = 2, 6, 10, 14, 18. b) The output currents when the unit number increases from 1 to 18. c) The transferred charges of the LS TENG network. d) The output charges when the unit number increases. All the TENG units are electrically connected in parallel. e) The voltage of a 10 mF capacitor when charged by an LS TENG network and used to power the radio frequency (RF) emitter. f) The illustration of the self-powered wireless SOS system for ocean emergency. The magnified current signals g) in the circuit and voltage h) of the 10 mF capacitor when powering the radio frequency device.

of the electrically parallel connecting, the average voltage hold almost constant when the unit number increases in Figure S6d in the Supporting Information. For further extension, when thousands of such TENGs are integrated as a network, a large quantity of blue energy from oceans will be harvested effectively and the “Blue-energy dream” will come true in the near future. The network of the LS TENGs can also be integrated with solar cell or others to harvest various kinds of energies.^[33,34]

2.5. A Self-Powered Wireless SOS System

Furthermore, we demonstrate a practical application of the LS TENGs as a self-powered wireless SOS system for emergencies, as presented in Figure 5e,f. The wireless SOS system contains a network of 18 LS TENGs, a bridge rectifier, a large capacitor, a wireless RF transmitter and receiver, shown in Figure S6g in the Supporting Information. The energy generated by the TENG is pulsed and unstable due to the uncontrollable and unstable environmental wave, therefore it should be stored by capacitor to provide a stable and manageable output and power the electronic devices. Then the wireless RF transmitter receives the energy from the capacitor and emits the signals wirelessly to an RF receiver, which is linked to a computer. The process could be seen in the Supporting Information as Movie 4. As exhibited in Figure 5e, the energy harvested by TENGs (a network of 18 PTFE films) can charge a 10 mF capacitor from 0 to 5 V in about 13 min, and then operate the wireless RF sensor. The voltage of the large capacitor rapidly descends to about 2.5 V as the RF sensor emits seven groups of 16 byte signals, which could be set as “SOS_SOS_SOS_SOS_” or others. And the magnified signal of Figure 5e is presented in Figure 5h, which clearly depicts that the voltage of the capacitor has 16 pulsed peaks when the RF sends a 16 byte signal. The current in the circuit also demonstrates 16 pulsed peaks when the RF sends the 16 byte signal as shown in Figure 5g.

3. Conclusion

A network of LS TENG is fabricated to efficiently harvest the huge quantities of blue energy from ocean. Due to the sufficient contact condition of the liquid–solid interface, the energy output per cycle of LS TENG is about 48.7 times bigger than that of the SS TENG with same area. The buoy-like LS TENG is especially suitable for efficiently harvesting low-frequency vibration energy. The output current, transferred charge, and the output voltage of the network of 18 LS TENGs are 290 μ A, 16 725 nC, and 300 V. And the SL TENG network can powder a wireless SOS system to emit the signals for ocean emergency. This study largely improves the efficiency of harvesting the blue energy and expands its application scope.

4. Experimental Section

Fabricating the Liquid–Solid Triboelectric Nanogenerator. The polymer films (PTFE, FEP, or PET) were cleaned with ethanol and pure water. Then they were dried by air gun. The metal electrode (Ag) was deposited

on the surface of polymer by magnetron sputtering. Different diameter (7.5 and 4 cm) of the 5 mm thick polymethyl methacrylate (PMMA) hollow cylinders were all cut to the length of 10 cm, while the diameter of 11 cm PMMA hollow cylinder was cut to 15 cm. The polymer films with the electrodes at their back side were attached to the surfaces of these cylinders. Finally these cylinders with polymer films were attached to be a concentric cylinder. When the inner liquid (pure water) and the aluminum foil (functioned as the bottom electrode) were put inside the concentric cylinder, a buoy-like liquid–solid triboelectric nanogenerator was completed.

Measuring the Triboelectric Nanogenerators's Outputs and the Wireless SOS System: The low noise current amplifier SR570 (Stanford Research System) was used to test the short-circuit currents, while the Keithley 6514 electrometer was used to measure the open-circuit voltage and transferred charge. The wireless SOS system contains a network of LS TENGs, a bridge rectifier, a large capacitor (10 mF), and a wireless radio frequency transmitter/receiver (nRF24L01P). The water waves in the aquarium were generated by the pump (Jebao ECO), which can control the movement and frequency of water, to simulate the marine environment.

Supporting Information

Supporting Information is available from the Wiley Online Library or from the author.

Acknowledgements

X.L. and J.T. contributed equally to this work. The research was supported by Chinese National Natural Science Foundation (Nos. 51622205, 61675027, 51432005, 61505010, 51502018, 11374174, 51390471, and 51527803); Beijing City Committee of Science and Technology (Z171100002017019), Beijing Natural Science Foundation (4181004), National 973 Project of China (2015CB654902); National key research and development project from Minister of Science and Technology, China (2016YFA0202703, 2016YFB0700402, and 2016YFA0302300); and the “Thousand Talents” program of China for pioneering researchers and innovative teams.

Conflict of Interest

The authors declare no conflict of interest.

Keywords

blue energy, liquid–solid interface, self-powered system, triboelectric nanogenerators

Received: March 4, 2018

Revised: March 27, 2018

Published online:

- [1] C. F. Pan, S. M. Niu, Y. Ding, L. Dong, R. M. Yu, Y. Liu, G. Zhu, Z. L. Wang, *Nano Lett.* **2012**, *12*, 3302.
- [2] L. Zhang, B. B. Zhang, J. Chen, L. Jin, W. L. Deng, J. F. Tang, H. T. Zhang, H. Pan, M. H. Zhu, W. Q. Yang, Z. L. Wang, *Adv. Mater.* **2016**, *28*, 1650.
- [3] R. J. Mehta, Y. L. Zhang, C. Karthik, B. Singh, R. W. Siegel, T. Borca-Tasciuc, G. Ramanath, *Nat. Mater.* **2012**, *11*, 233.
- [4] C. F. Pan, Z. T. Li, W. X. Guo, J. Zhu, Z. L. Wang, *Angew. Chem., Int. Ed.* **2011**, *50*, 11192.

- [5] J. H. Lee, J. Kim, T. Y. Kim, M. S. Al Hossain, S. W. Kim, J. H. Kim, *J. Mater. Chem. A* **2016**, *4*, 7983.
- [6] J. E. Trancik, *Nature* **2014**, *507*, 300.
- [7] G. B. Xue, Y. Xu, T. P. Ding, J. Li, J. Yin, W. W. Fei, Y. Z. Cao, J. Yu, L. Y. Yuan, L. Gong, J. Chen, S. Z. Deng, J. Zhou, W. L. Guo, *Nat. Nanotechnol.* **2017**, *12*, 317.
- [8] J. D. Feng, M. Graf, K. Liu, D. Ovchinnikov, D. Dumcenco, M. Heiraniyan, V. Nandigana, N. R. Aluru, A. Kis, A. Radenovic, *Nature* **2016**, *536*, 197.
- [9] Z. L. Wang, *Nature* **2017**, *542*, 159.
- [10] X. Y. Li, J. A. Tao, W. X. Guo, X. J. Zhang, J. J. Luo, M. X. Chen, J. Zhu, C. F. Pan, *J. Mater. Chem. A* **2015**, *3*, 22663.
- [11] S. H. Kim, C. S. Haines, N. Li, K. J. Kim, T. J. Mun, C. Choi, J. T. Di, Y. J. Oh, J. P. Oviedo, J. Bykova, S. L. Fang, N. Jiang, Z. F. Liu, R. Wang, P. Kumar, R. Qiao, S. Priya, K. Cho, M. Kim, M. S. Lucas, L. F. Drummy, B. Maruyama, D. Y. Lee, X. Lepro, E. L. Gao, D. Albarq, R. Ovalle-Robles, S. J. Kim, R. H. Baughman, *Science* **2017**, *357*, 773.
- [12] X. F. Wang, S. M. Niu, Y. J. Yin, F. Yi, Z. You, Z. L. Wang, *Adv. Energy Mater.* **2015**, *5*, 1501467.
- [13] J. Chen, J. Yang, Z. L. Li, X. Fan, Y. L. Zi, Q. S. Jing, H. Y. Guo, Z. Wen, K. C. Pradel, S. M. Niu, Z. L. Wang, *ACS Nano* **2015**, *9*, 3324.
- [14] T. Jiang, Y. Y. Yao, L. Xu, L. M. Zhang, T. X. Xiao, Z. L. Wang, *Nano Energy* **2017**, *31*, 560.
- [15] X. J. Zhao, G. Zhu, Y. J. Fan, H. Y. Li, Z. L. Wang, *ACS Nano* **2015**, *9*, 7671.
- [16] X. Y. Li, J. Tao, J. Zhu, C. F. Pan, *APL Mater.* **2017**, *5*, 074104.
- [17] C. S. Wu, R. Y. Liu, J. Wang, Y. L. Zi, L. Lin, Z. L. Wang, *Nano Energy* **2017**, *32*, 287.
- [18] Y. Xi, H. Y. Guo, Y. L. Zi, X. G. Li, J. Wang, J. N. Deng, S. M. Li, C. G. Hu, X. Cao, Z. L. Wang, *Adv. Energy Mater.* **2017**, *7*, 1602397.
- [19] H. S. Wang, C. K. Jeong, M. H. Seo, D. J. Joe, J. H. Han, J. B. Yoon, K. J. Lee, *Nano Energy* **2017**, *35*, 415.
- [20] R. J. Davey, L. Williams-Seton, H. F. Lieberman, N. Blagden, *Nature* **1999**, *402*, 797.
- [21] G. Zhu, Y. J. Su, P. Bai, J. Chen, Q. S. Jing, W. Q. Yang, Z. L. Wang, *ACS Nano* **2014**, *8*, 6031.
- [22] G. T. Hwang, V. Annapureddy, J. H. Han, D. J. Joe, C. Baek, D. Y. Park, D. H. Kim, J. H. Park, C. K. Jeong, K. I. Park, J. J. Choi, D. K. Kim, J. Ryu, K. J. Lee, *Adv. Energy Mater.* **2016**, *6*, 1600237.
- [23] L. Xu, Y. K. Pang, C. Zhang, T. Jiang, X. Y. Chen, J. J. Luo, W. Tang, X. Cao, Z. L. Wang, *Nano Energy* **2017**, *31*, 351.
- [24] S. F. L. Mertens, A. Hemmi, S. Muff, O. Groning, S. De Feyter, J. Osterwalder, T. Greber, *Nature* **2016**, *534*, 676.
- [25] W. Tang, T. Jiang, F. R. Fan, A. F. Yu, C. Zhang, X. Cao, Z. L. Wang, *Adv. Funct. Mater.* **2015**, *25*, 3718.
- [26] Z. H. Lin, G. Cheng, L. Lin, S. Lee, Z. L. Wang, *Angew. Chem., Int. Ed.* **2013**, *52*, 12545.
- [27] C. Zhang, J. Li, C. B. Han, L. M. Zhang, X. Y. Chen, L. D. Wang, G. F. Dong, Z. L. Wang, *Adv. Funct. Mater.* **2015**, *25*, 5625.
- [28] X. Y. Li, M. X. Chen, R. M. Yu, T. P. Zhang, D. S. Song, R. R. Liang, Q. L. Zhang, S. B. Cheng, L. Dong, A. L. Pan, Z. L. Wang, J. Zhu, C. F. Pan, *Adv. Mater.* **2015**, *27*, 4447.
- [29] X. Y. Li, R. L. Liang, J. Tao, Z. C. Peng, Q. M. Xu, X. Han, X. D. Wang, C. F. Wang, J. Zhu, C. F. Pan, *ACS Nano* **2017**, *11*, 3883.
- [30] M. X. Chen, X. Y. Li, L. Lin, W. M. Du, X. Han, J. Zhu, C. F. Pan, Z. L. Wang, *Adv. Funct. Mater.* **2014**, *24*, 5059.
- [31] X. D. Wang, M. L. Que, M. X. Chen, X. Han, X. Y. Li, C. F. Pan, Z. L. Wang, *Adv. Mater.* **2017**, *29*, 1706738.
- [32] W. X. Guo, X. Y. Li, M. X. Chen, L. Xu, L. Dong, X. Cao, W. Tang, J. Zhu, C. J. Lin, C. F. Pan, Z. L. Wang, *Adv. Funct. Mater.* **2014**, *24*, 6691.
- [33] Y. Zhang, R. D. Cong, W. Zhao, Y. Li, C. H. Jin, W. H. Yu, G. S. Fu, *Sci. Bull.* **2016**, *61*, 787.
- [34] N. L. Yang, *Sci. Bull.* **2017**, *62*, 234.
- [35] Y. L. Zi, J. Wang, S. H. Wang, S. M. Li, Z. Wen, H. Y. Guo, Z. L. Wang, *Nat. Commun.* **2016**, *7*, 10987.
- [36] Y. L. Zi, S. M. Niu, J. Wang, Z. Wen, W. Tang, Z. L. Wang, *Nat. Commun.* **2015**, *6*, 8376.
- [37] Y. L. Zi, H. Y. Guo, J. Wang, Z. Wen, S. M. Li, C. G. Hu, Z. L. Wang, *Nano Energy* **2017**, *31*, 302.